RSC Advances

Podophyllotoxin–pterostilbene fused conjugates as potential multifunctional antineoplastic agents against human uveal melanoma cells

Lei Zhang,*[a] Jing Wang,*[a] Lai Liu,[a] Chengyue Zheng,[a] Yang Wang,[a] Yongzheng Chen[a] and Gang Wei[b]

Uveal melanoma is the most common primary intraocular malignancy with a high tendency for early metastasis. There is an urgent need for novel anticancer agents for the therapy of uveal melanoma. In this paper, two novel conjugates of podophyllotoxin–pterostilbene were prepared and evaluated for their cytotoxicity against human uveal melanoma cells (MUM-2B and C918) by the CCK-8 assay. Conjugate **B1** exhibited a significant IC_{50} value of 0.081 ± 0.004 µM against MUM-2B cells. Treatment of MUM-2B cells with **B1** caused S cell cycle arrest through reductions in CyclinB1, CDK1 and CDK2 levels. In addition, **B1** showed antimigratory activity by down-regulating the expression of VEGFR-2 and MMP-2, and up-regulating the level of E-cadherin. Furthermore, **B1** treatment resulted in the induction of apoptosis as characterized by Hoechst 33342 staining, flow cytometry and cleavage of procaspases-3, -8, and -9. Finally, **B1** significantly inhibited TOPOIIα and TOPOIIβ expression, simultaneously suppressing the ERK1/2 and AKT pathways in MUM-2B cells.

Introduction

Uveal melanoma, a rare form of melanoma, is the most frequent primary intraocular malignancy in adults.[1] Unfortunately, uveal melanoma has a high tendency for early metastasis, especially spreading hematogenously to the liver.[2] Meanwhile, uveal melanoma cells are highly resistant to antineoplastic drugs.[3] Untill now, there are lack of effective treatments for uveal melanoma. Therefore, there is an urgent need for novel anticancer agents for the therapy of uveal melanoma patients.[4]

Natural products have been widely and successfully used in treating multiple diseases, such as carcinoma.[5,6] Podophyllotoxin (PPT, **1**, Fig. 1), a well-known non-alkaloid toxin lignan exhibiting

great anti-tumor activity by inhibiting tubulin polymerization,[7] is isolated from *Podophyllum hexandrum*.[8,9] However, due to unacceptable toxic side effects (*e.g.*, myelosuppression, liver injury and neutropenia), it is unable to be applied in cancer treatment.[10] To overcome the faults, numerous structural modifications of podophyllotoxin have been undertaken to generate some analogs with better pharmacological characters,[11] such as etoposide (**2**, Fig. 1) and teniposide (**3**, Fig. 1), which are used for the treatment of small-cell lung cancer, leukaemia, neuroblastoma and non-Hodgkin's lymphoma.[12] In recent years, hundreds of derivatives have been synthesized from the skeleton of PPT, with higher antineoplastic profiles, such as GL-331, QS-ZYX-1-61 and Taflu-poside.[13] Notably, several researchers showed that PPT and its derivatives presented cytotoxicity in skin melanoma. For instance, Kamal *et al.* reported that PPT and its derivatives displayed significant antiproliferative activity against A375 and B16 skin melanoma cells.[14,15] However, whether PPT and its derivatives exert antitumor effect in uveal melanoma remains unclear.

Inspired by the molecules hybridization concept,[16] in this study, we described the design of two novel podophyllotoxin conjugates, with the natural product pterostilbene (*trans*-3,5-dimethoxy-4′-hydroxystilbene, PTS, **4**, Fig. 2),[17,18] a dimethylated analog of resveratrol (**5**, Fig. 2). PTS, existed in many fruits (such as blueberries and vaccinium berries), showed diverse pharmacological properties,[19–24] including anticancer, antioxidant, antidiabetic, hypolipidemic activities and anti-inflammation. It was further confirmed that PTS had no toxic effect on mice at high does.[25] Additionally, previous studies reported that PTS possessed anticarcinogenic activity against skin melanoma cells.[26,27]
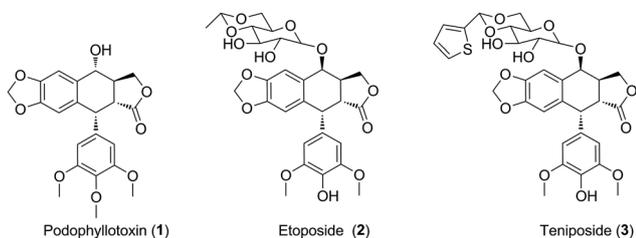

Fig. 1 The structures of podophyllotoxin and its analogues.

[a]*School of Pharmacy, Zunyi Medical University, 201 Dalian Road, Zunyi 563003, P. R. China. E-mail: lzhang@zmc.edu.cn; wangjing@zmc.edu.cn*

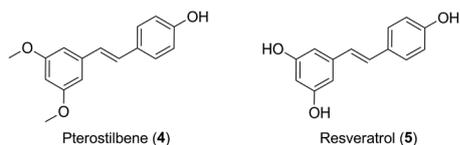[b]*CSIRO Manufacturing Flagship, PO Box 218, Lindfield, NSW 2070, Australia*

Fig. 2   Examples of pterostilbene and resveratrol.
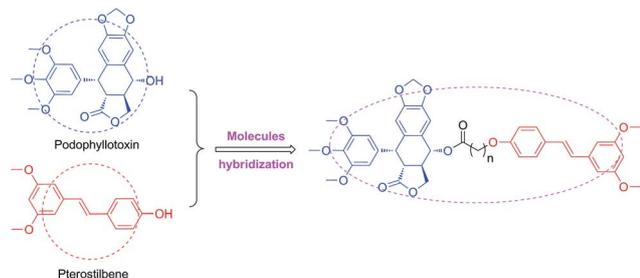
Pterostilbene (4)   Resveratrol (5)

Fig. 3   Design of targeted molecules.

It's well known that PPT shows significant cytotoxicity in both of cancer and normal cells. Therefore, it is an urgent need to solve the toxicity issue of PPT. To reduce the toxicity of PPT and find new multifunctional antineoplastic agents based on the PPT skeleton in our group,[28–30] here we reported the design, synthesis and antiproliferative activity of novel podophyllotoxin–pterostilbene conjugates using molecules hybridization (Fig. 3) in human uveal melanoma cells (MUM-2B and C918), simultaneously, the underlying molecular mechanisms were also investigated.

Results and discussion

The hybrid compounds (**B1** and **B2**) were synthesized as shown in Scheme 1. Firstly, **PPT** was reacted with chloroacetyl chloride or 3-chloropropionyl chloride to provide the intermediates **6** or **7**. Then, compounds **6** or **7** were reacted with **PTS** in the presence of potassium carbonate and potassium iodide to give the target molecules **B1** or **B2**. The structures of podophyllotoxin–pterostilbene conjugates were confirmed by ^{1}H NMR, ^{13}C NMR and HR-MS.

The novel podophyllotoxin–pterostilbene conjugates **B1** and **B2** were tested by CCK-8 assay for their *in vitro* antineoplastic
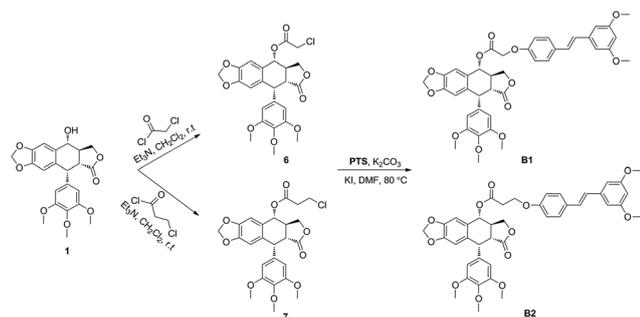
Scheme 1   Synthesis of podophyllotoxin–pterostilbene conjugates.

Table 1 Antiproliferative activity of the podophyllotoxin–pterostilbene conjugates

Compound	IC$_{50}$^{a} (μM)		
	MUM-2B	C918	HUVEC
B1	0.081 ± 0.004	0.347 ± 0.054	0.362 ± 0.109
B2	0.613 ± 0.307	1.035 ± 0.152	2.265 ± 0.862
PPT	0.016 ± 0.006	0.012 ± 0.002	0.018 ± 0.008
PTS	40.314 ± 9.862	68.124 ± 7.422	80.809 ± 15.742
Etoposide	1.965 ± 0.221	1.279 ± 0.221	2.255 ± 0.224

^{a} Data were expressed as mean IC$_{50}$ ± SD (μM) from three independent experiments.

activity against human uveal melanoma cells (MUM-2B and C918) and human umbilical vein endothelial cells (HUVEC). **PPT**, **PTS** and clinical drug etoposide were used as positive compounds. The results were summarized in Table 1. All tested molecules displayed potent cytotoxicity. Positive compound **PPT** exhibited nonspecific cytotoxicity against MUM-2B, C919 and HUVEC cells with IC$_{50}$ values of 0.016 ± 0.006, 0.012 ± 0.002 and 0.018 ± 0.008 μM, respectively, which showed that **PPT** not only had strong antiproliferative activity, but also possessed high toxicity. In addition, **PTS** showed weaker cytotoxic activity than etoposide against above three cells with IC$_{50}$ values ranging from 40.314 ± 9.862 to 80.809 ± 15.742 μM. Interesting, hybrid compounds **B1** and **B2** showed significant antiproliferative activity compared with **PTS**. Our data showed that conjugates **B1** and **B2** displayed less cytotoxic activity than **PPT**, which may be involved with the solubility property. In addition, **B1** showed better anticancer effect against MUM-2B (0.081 ± 0.004 μM) than C918 cells (0.347 ± 0.054 μM), showing 497- and 196-fold more cytotoxic than that of **PTS** (40.314 ± 9.862 and 68.124 ± 7.422 μM), respectively. Moreover, the IC$_{50}$ value of **B1** against human normal HUVEC cells was 0.362 ± 0.109 μM which was less cytotoxicity than that of **PPT**, indicating that conjugate had less toxicity. From the data of **B1** and **B2**, conjugate displayed less anticancer activity with longer linker, at the same time, exhibited less toxicity. It was found that MUM-2B cells were more sensitive to conjugate as well as **PTS** than C918 cells. Furthermore, the solubility property and more details in the structure–activity relationship need further study.

To investigate the effect of **B1** on the cell cycle, MUM-2B cells were treated with 0.1 μM **B1** for 48 h, and then analyzed by flow cytometry. **PPT** and **PTS** were used as positive compounds. As shown in Fig. 4, after treatment with 0.1 μM **B1**, 77.69% of cell numbers were accumulated in S phase, compared with 16.54% cells accumulation in S phase in control group. Meanwhile, the percentages of cells in S phase were 81.42% and 74.11%, respectively, in 0.01 μM **PPT** and 50 μM **PTS**-treated groups. It was revealed that conjugate **B1** could induce MUM-2B cells arrest at S phase.

Next, to validate whether the inhibitory effect of **B1** on MUM-2B cells proliferation are accompanied by apoptosis, MUM-2B cells were treated with 0.1 μM **B1** for 48 h, and the apoptotic cells were analyzed by flow cytometry. **PPT** and **PTS** were used as positive compounds. We observed that the rate of apoptosis
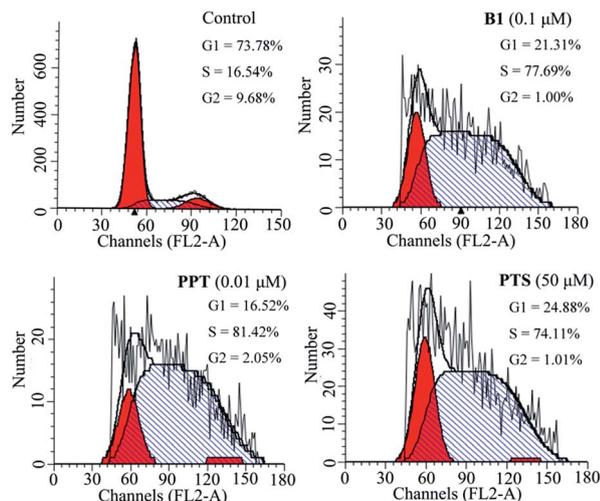
Fig. 4   Effects of conjugate B1, PPT and PTS on the cycle of MUM-2B cells. Cells were treated with vehicle, 0.1 μM B1, 0.01 μM PPT or 50 μM PTS for 48 h.

in 0.1 μM B1-treated group was 37.72% (Fig. 5), which were stronger than that of the control group (4.16%). Similarly, apoptotic cell number increased to 32.95% and 48.73% when the cells were incubated with 0.01 μM PPT and 50 μM PTS, respectively. These results indicated that conjugate B1 could induce apoptosis in MUM-2B cells.

Furthermore, to confirm the induction of apoptosis of B1, MUM-2B cells were tested by Hoechst 33342 staining. As seen in Fig. 6, treatment with 0.1 μM B1 led to cell shrinkage and chromatin condensation. Meanwhile, bright blue fluorescent and condensed nuclei in apoptosis cells were observed by treatment with 0.1 μM B1. Similar effects were observed when cells were incubated with 0.01 μM PPT and 50 μM PTS. There were no significant characteristics of apoptosis in
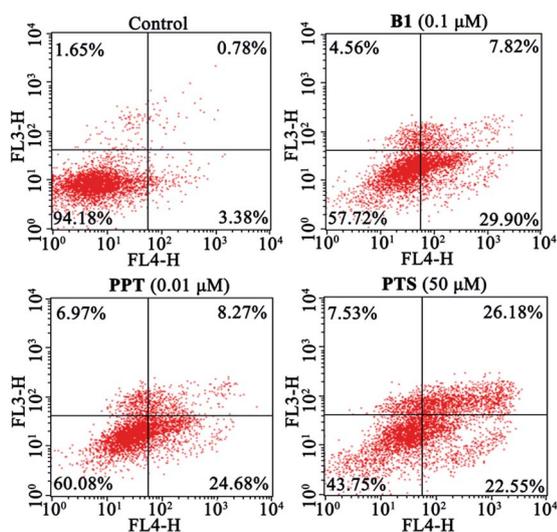
control group. The above results significantly proved that conjugate B1 was effective in inducing MUM-2B cells apoptosis.

Recently, some studies reported that PPT and PTS both had the potential to suppress tumor migratory and metastasis.[31–33] To further test the effect of conjugate B1 on the migration potential of cancer cells, wound healing assay was conducted on MUM-2B cells in vitro. As shown in Fig. 7, after treatment with 0.1 μM B1, 0.01 μM PPT or 50 μM PTS for 24 h, the migration of MUM-2B cells was suppressed obviously, compared with the control group. These data indicated that conjugate B1 might have the potential to inhibit the migratory and metastasis of MUM-2B cells.

To evaluate the mechanisms involved in S cell cycle arrest in MUM-2B cells, the effects of B1 on expression of cell cycle-related proteins were examined by western blotting using PPT and PTS as positive compounds. As shown in Fig. 8A, 0.1 μM B1 significantly decreased the expression levels of CDK1, CDK2 and CyclinB1, compared with the vehicle-treated control, however, CyclinA level in MUM-2B cells was not changed. Similar effects were observed when cells were incubated with 0.01 μM PPT and 50 μM PTS. Taken together, these data proved that conjugate B1 blocked MUM-2B cells in the S phase by down-regulation of CDK1, CDK2 and CyclinB1.

In order to further investigate the mechanisms involved in apoptosis induced by B1, the expression of apoptotic proteins (the cleavage states of caspase 3, 8 and 9) in MUM-2B cells was examined by western blotting (Fig. 8B). PPT and PTS were used as positive compounds. The data revealed that 0.1 μM B1-treatment dramatically increased the relative levels of cleaved caspase 3, 8 and 9 in MUM-2B cells. Similar effects were observed when cells were incubated with 0.01 μM PPT and 50 μM PTS. Collectively, these findings strongly demonstrated that conjugate B1-induced apoptosis of MUN-2B cells was mediated by signaling cascade of apoptosis.

Our above findings showed that conjugate B1 possessed antimigratory activity in MUM-2B cells. Furthermore, Vascular Endothelial Growth Factor Receptor 2 (VEGFR-2), Matrix Metalloproteinase-2 (MMP-2) and E-cadherin are crucial events of invasion and metastasis in malignant cancer cells.[34–36] Thus, we next further assess the roles of above metastasis-related proteins in B1-treated MUM-2B cells by western blotting. As shown in Fig. 9A, treatment with 0.1 μM B1 significantly increased the expression level of E-cadherin, simultaneously, down-regulated the levels of VEGFR-2 and MMP-2 in MUM-2B cells, compared with the control group. Interestingly, the levels of VEGFR-2 and E-cadherin were not altered by 0.01 μM PPT, whereas, 50 μM PTS did, suggesting that the antimigratory activity of B1 was related with the structure of PTS. These findings suggested that the anti-migratory effect of conjugate B1 was mediated by VEGFR-2, MMP-2 and E-cadherin.

Ren et al. demonstrated that PPT derivative could inhibit the expression of DNA topoisomerase IIα in HepG2 cells.[37] Consequently, we next investigated the effects of B1 on the DNA topoisomerase IIα (TOPOIIα) and DNA topoisomerase IIβ
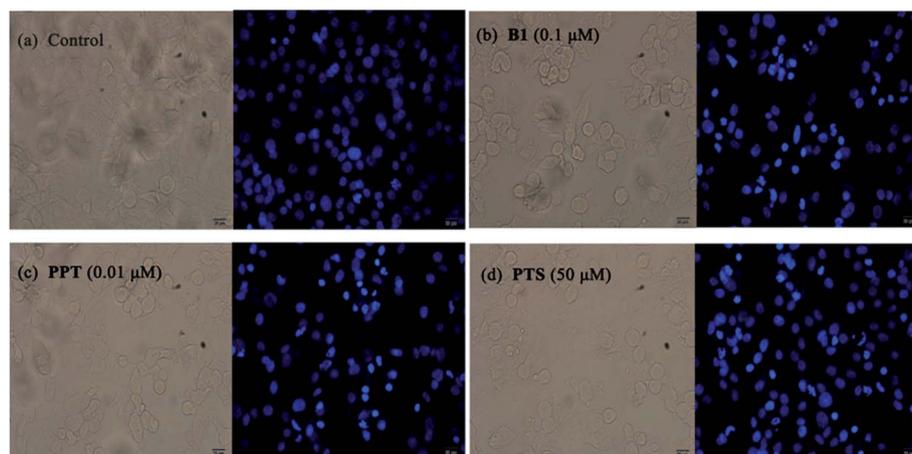

Fig. 5   Effects of conjugate B1, PPT and PTS on the apoptosis of MUM-2B cells. Cells were treated with vehicle, 0.1 μM B1, 0.01 μM PPT or 50 μM PTS for 48 h.

Fig. 6 Effects of conjugate **B1**, **PPT** and **PTS** on the morphology of MUM-2B cells. Cells were treated with vehicle, 0.1 μM **B1**, 0.01 μM **PPT** or 50 μM **PTS** for 24 h, then stained with Hoechst 33342 for microscopy. (a) Control group; (b) 0.1 μM **B1**; (c) 0.01 μM **PPT**; (d) 50 μM **PTS**. Magnification: 200×, scale 20 μm.
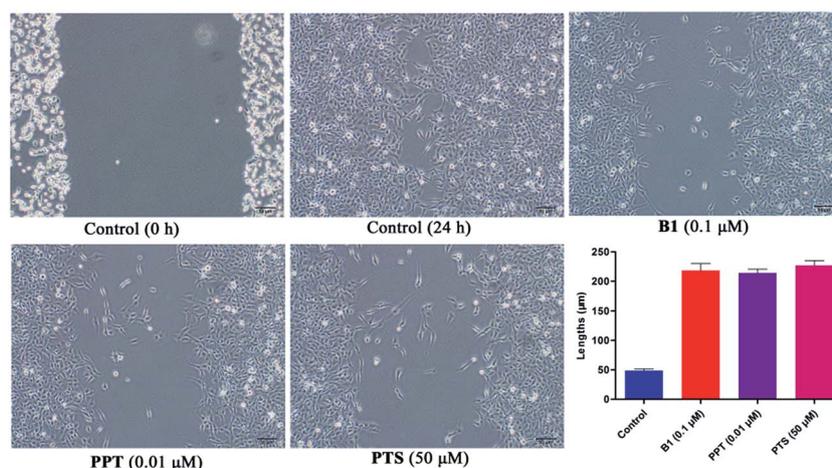

Fig. 7 Effects of conjugate **B1**, **PPT** and **PTS** on the migration of MUM-2B cells *in vitro*. Cells were treated with vehicle, 0.1 μM **B1**, 0.01 μM **PPT** or 50 μM **PTS** for 24 h. Columns mean and bars given here follow ±SD of three independent experiments. Magnification: 100×, scale 50 μm.

(TOPOIIβ) proteins expression by western blotting. As shown in Fig. 9B, 0.1 μM **B1** demonstrated the ability to decrease the expression of TOPOIIα and TOPOIIβ in MUM-2B cells. Similar effect was observed when cells were incubated with 0.01 μM **PPT**. Interestingly, 50 μM **PTS** could down-regulate the TOPOIIα expression level, while, increase the expression of TOP-OIIβ. Collectively, the results indicated that conjugate **B1** could lower the expression levels of TOPOIIα and TOPOIIβ in MUM-2B cells.

It was reported that **PTS** showed anti-inflammatory and anticarcinogenic activity by inhibition of COX-2 and iNOS.[38–40] Thus, the expression of inflammatory-related proteins in **B1**-treated MUM-2B cells was performed by western blotting. As seen in Fig. 9C, treatment with 0.01 μM **B1** could not alter the expression levels of COX-2 and iNOS in MUM-2B cells. Similar effect was observed in 0.01 μM **PPT** group. However, 50 μM **PTS** could down-regulate the COX-2 level. The results confirmed that

the cytotoxic activity of conjugate **B1** against MUM-2Bcells might not be mediated by COX-2 and iNOS.

More recently, we showed that **PPT** and its analogue could stimulate the ERK1/2 pathway in K562/adr cells.[41] To further clarify the molecular mechanisms underlying the activity of **B1**, we finally investigated the effects of **B1** on the ERK1/2, AKT and STAT3 signaling in MUM-2B cells. Cells were treated with vehicle, 0.1 μM **B1**, 0.01 μM **PPT** or 50 μM **PTS** for 48 h. Phosphorylation of ERK1/2, AKT and STAT3 was determined by western blotting. Fig. 10 showed that treatment with 0.1 μM **B1** significantly suppressed the phosphorylation of ERK1/2 and AKT in MUM-2B cells, however, the phosphorylation of STAT3 was not altered, compared with the control group. Similar effects were observed when cells were treated with 0.01 μM **PPT** and 50 μM **PTS**. These results suggested that conjugate **B1** might inhibit the activation of the ERK1/2 and AKT pathways, which contributed to its antineoplastic activity in MUM-2B cells.
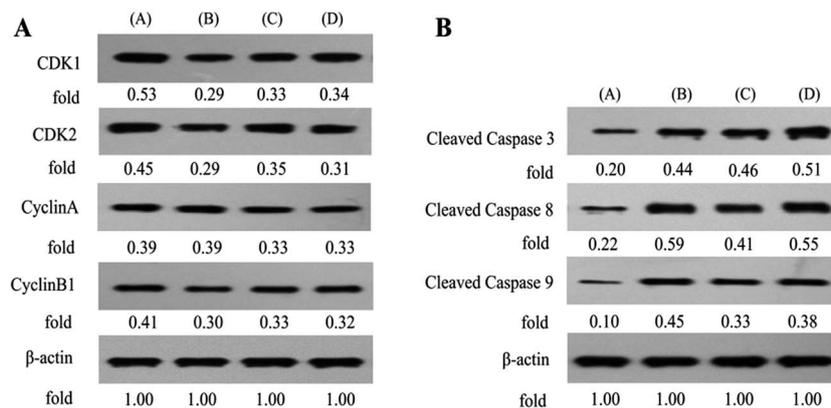
Fig. 8 Effects of conjugate **B1**, **PPT** and **PTS** on the cell cycle- and apoptosis-related proteins expression, respectively, in MUM-2B cells by western blotting using β-actin as a control. (A) Control MUM-2B cells; (B) MUM-2B cells treated with 0.1 μM **B1**; (C) MUM-2B cells treated with 0.01 μM **PPT**; (D) MUM-2B cells treated with 50 μM **PTS**.
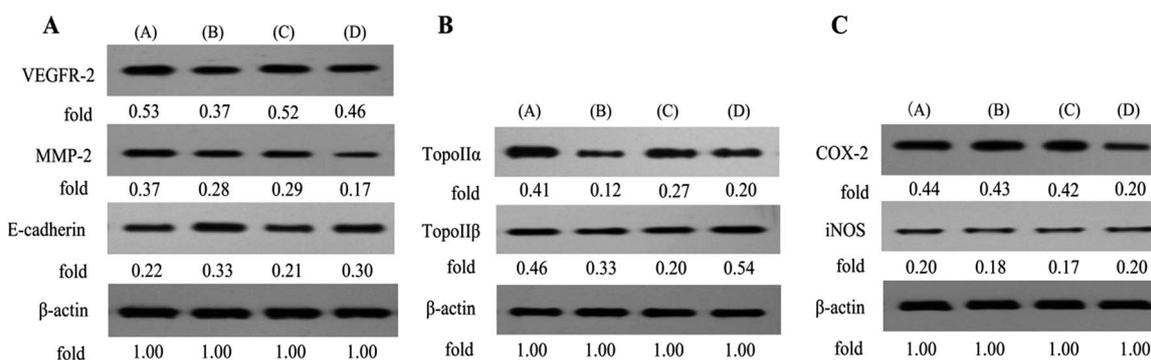
Fig. 9 Effects of conjugate **B1**, **PPT** and **PTS** on the metastasis-, TOPO- and inflammatory-related proteins expression, respectively, in MUM-2B cells by western blotting using β-actin as a control. (A) Control MUM-2B cells; (B) MUM-2B cells treated with 0.1 μM **B1**; (C) MUM-2B cells treated with 0.01 μM **PPT**; (D) MUM-2B cells treated with 50 μM **PTS**.

Fig. 10 Effects of conjugate **B1**, **PPT** and **PTS** on the ERK1/2, AKT and STAT3 signaling in MUM-2B cells by western blotting using β-actin as a control. (A) Control MUM-2B cells; (B) MUM-2B cells treated with 0.1 μM **B1**; (C) MUM-2B cells treated with 0.01 μM **PPT**; (D) MUM-2B cells treated with 50 μM **PTS**.
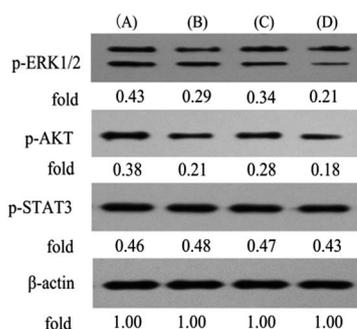
Experimental

General

Melting points were taken on a SGWX-4 meltingpoint apparatus. High-resolution mass spectra (HR-MS) were performed on an Agilent Accurate-Mass-Q-TOF-MS 6520. The ^{1}H and ^{13}C NMR spectra were recorded on an Agilent-NMR-vnmrs (400 MHz) instrument using TMS as internal standard.

Preparation of intermediates 6 and 7

To a solution of **PPT** (1.9 mmol, 1 eq.) and triethylamine (4 eq.) in dry dichloromethane (15 mL) for at 0 °C, chloroacetyl chloride or 3-chloropropionyl chloride (2.5 eq.) was added. The mixture was stirred under argon at room temperature for 1 h. After that, the mixture was quenched with NH_4Cl (5 mL) for 10 min and extracted with dichloromethane (3 × 10 mL). The combined organic phase was washed with brine, then dried over anhydrous $MgSO_4$ and evaporated under reduced pressure. The crude was further purified by column chromatography (dichloromethane/methanol = 100 : 1) to give the intermediate.

Chloroacetate-4-desoxypodophyllotoxin (6). Yellowish white power, yield 90%; mp: 219–220 °C; ^{1}H NMR (400 MHz, CDCl$_3$) δ 6.77 (s, 1H), 6.55 (s, 1H), 6.37 (s, 2H), 5.99 (d, J = 4.8 Hz, 2H), 5.96 (d, J = 8.4 Hz, 1H), 4.61 (d, J = 2.6 Hz, 1H), 4.38–4.42 (m, 1H), 4.13–4.24 (m, 3H), 3.80 (s, 3H), 3.75 (s, 6H), 2.84–2.97 (m, 2H); ^{13}C NMR (100 MHz, CDCl$_3$) δ 173.41, 167.94, 152.65, 148.41, 147.70, 137.11, 134.53, 132.55, 127.21, 109.78, 107.97,
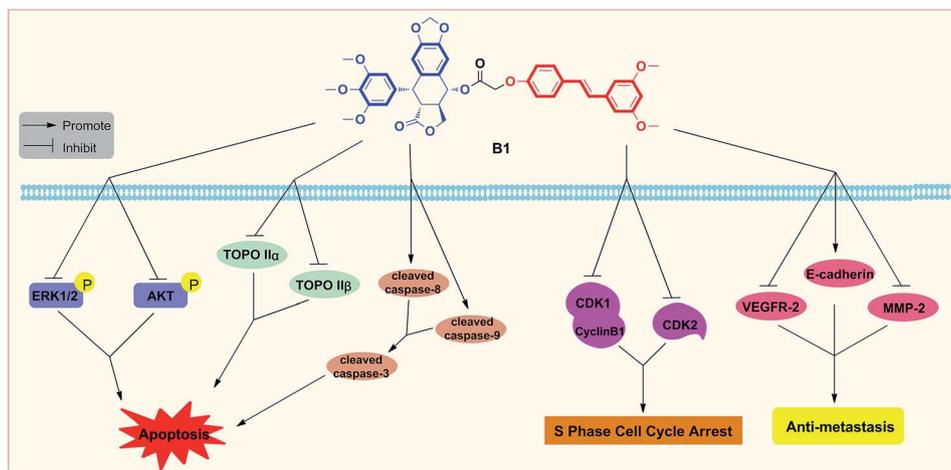
Fig. 11 Proposed diagrams of antineoplastic activity of conjugate **B1** against human uveal melanoma MUM-2B cells.

106.92, 101.71, 75.64, 71.13, 60.75, 56.13, 45.52, 43.64, 40.69, 40.48, 38.46; HRMS-ESI (m/z): calcd for $C_{24}H_{27}NClO_9$ $[M + NH_4]^+$ 508.1369, found 508.1367.

3-Chloropropionate-4-desoxypodophyllotoxin (7). Yellowish white power, yield 84%; mp: 139–141 °C; ^1H NMR (400 MHz, CDCl$_3$) δ 6.79 (s, 1H), 6.55 (s, 1H), 6.50 (d, $J = 17.2$ Hz, 1H), 6.40 (d, $J = 4.8$ Hz, 2H), 6.20 (dd, $J = 10.4, 17.2$ Hz, 1H), 6.00 (s, 1H), 5.98 (s, 2H), 5.95 (s, 1H), 4.62 (d, $J = 4.0$ Hz, 1H), 4.40 (dd, $J = 7.2, 9.6$ Hz, 1H), 4.24 (t, $J = 9.2$ Hz, 1H), 3.81 (s, 3H), 3.76 (s, 6H), 2.98–2.91 (m, 2H); ^{13}C NMR (100 MHz, CDCl$_3$) δ 173.66, 166.42, 152.60, 148.15, 147.60, 134.79, 132.39, 128.19, 127.65, 109.72, 107.98, 107.06, 101.61, 73.72, 71.40, 60.76, 56.15, 56.10, 45.60, 43.72, 38.72; HRMS-ESI (m/z): calcd for $C_{25}H_{29}NClO_9$ $[M + NH_4]^+$ 522.1525, found 522.1523.

Preparation of target compounds B1 and B2

To a solution of **6** or **7** (0.25 mmol, 1 eq.), potassium iodide (0.01 eq.), potassium carbonate (1 eq.) in DMF (4 mL), **PTS** (1.1 eq.) was added, and the reaction mixture was stirred under argon at 80 °C for 1 h. The reaction mixture was cooled, added to water, and extracted with dichloromethane (3 × 10 mL). The combined organic phase was washed with brine, then dried over anhydrous MgSO$_4$ and evaporated under reduced pressure. The crude was further purified by column chromatography (ethyl acetate/petroleum ether = 1 : 2–1 : 4) to give targeted molecule.

(E)-4-(3,5-Dimethoxystyryl)phenyl acetate-4-desoxypodophyllotoxin (B1). White power, yield 62%; mp: 104–105 °C; ^1H NMR (400 MHz, CDCl$_3$) δ 7.45 (d, $J = 8.8$ Hz, 2H), 7.02 (d, $J = 16.4$ Hz, 1H), 6.91 (d, $J = 16.4$ Hz, 1H), 6.89 (d, $J = 8.4$ Hz, 2H), 6.64 (s, 3H), 6.52 (s, 1H), 6.34–6.38 (m, 3H), 5.98 (d, $J = 8.4$ Hz, 2H), 5.96 (s, 1H), 4.78 (d, $J = 4.8$ Hz, 2H), 4.59 (d, $J = 3.6$ Hz, 1H), 4.36–4.32 (m, 1H), 4.19 (t, $J = 9.2$ Hz, 1H), 3.82 (s, 6H), 3.80 (s, 3H), 3.74 (s, 6H), 2.93–2.80 (m, 2H); ^{13}C NMR (100 MHz, CDCl$_3$) δ 173.40, 169.53, 160.94, 157.12, 152.63, 148.30, 147.61, 139.35, 137.09, 134.63, 132.45, 131.38, 128.19, 127.95, 127.44, 127.38, 114.66, 109.74, 107.97, 106.88, 104.37, 101.68, 99.74, 74.79, 71.11, 65.26, 60.76, 56.14,

55.36, 45.45, 43.63, 38.49; HRMS-ESI (m/z): calcd for $C_{40}H_{39}O_{12}$ $[M + H]^+$ 711.2436, found 711.2434.

(E)-4-(3,5-Dimethoxystyryl)phenyl propionate-4-desoxypodophyllotoxin (B2). White power, yield 57%; mp: 205–207 °C; ^1H NMR (400 MHz, CDCl$_3$) δ 6.79 (s, 2H), 6.56 (s, 2H), 6.37 (s, 3H), 6.26 (d, $J = 17.2$ Hz, 2H), 5.97 (s, 2H), 5.95 (s, 2H), 5.84 (s, 1H), 5.81 (s, 1H), 5.79 (s, 1H), 4.47–4.41 (m, 3H), 4.30 (d, $J = 3.2$ Hz, 1H), 4.27 (d, $J = 2.8$ Hz, 1H), 3.82 (s, 6H), 3.77 (s, 9H), 3.33 (dd, $J = 3.2, 9.2$ Hz, 2H), 3.08–3.02 (m, 2H); ^{13}C NMR (100 MHz, CDCl$_3$) δ 177.38, 165.59, 153.19, 148.47, 147.22, 138.95, 136.71, 132.19, 131.22, 127.61, 126.02, 109.90, 108.68, 105.22, 101.43, 72.49, 70.75, 60.81, 56.11, 45.35, 44.29, 39.61, 29.68; HRMS-ESI (m/z): calcd for $C_{41}H_{41}O_{12}$ $[M + H]^+$ 725.2593, found 725.2589.

Pharmacology

Materials. DMSO, antibodies (except TopoIIα and TopoIIβ), cells, PBS, CCK-8, apoptosis detection kit, cell cycle detection kit and Hoechst 33342 were purchased from KeyGen Biotech (Nanjing, China). TopoIIα and TopoIIβ were purchased from Proteintech Group (Chicago, IL). FBS was bought from ExCell Biology (Shanghai, China).

CCK-8 assay.[42] MUM-2B, C918 or HUVEC cells were planted in 96-well plates for 24 h, and then incubated with 0.1% DMSO and test compounds at the indicated concentration for 72 h at 37 °C. Then, cells were incubated CCK-8 (10 μL) for 2 h. The absorbance was determinated at 450 nm.

Cell cycle analysis.[42] MUM-2B cells were plated in 6-well plates for 12 h, and then incubated with 0.1% DMSO and test compounds at the indicated concentration for 48 h. Then, cells were harvested and fixed overnight in 70% ethanol at 4 °C. Subsequently, cells were washed three times with PBS, and then incubated with RNase (100 μL) at 37 °C for 30 min and stained with propidium iodide (400 μL) at 4 °C for 30 min. The cells were measured by a flow cytometer.

Cell apoptosis assay.[42] MUM-2B cells were plated in 6-well plates for 12 h, and then incubated with 0.1% DMSO and test compounds at the indicated concentration for 48 h. Subsequently, cells were washed twice with PBS, and then treated with Annexin

V-APC (5 μL) and 7-AAD (5 μL) at room temperature for 15 min in the dark. Apoptotic cells were quantified using a flow cytometer.

Hoechst 33242 staining.[42] MUM-2B cells incubated with 0.1% DMSO and test compounds at the indicated concentration for a period of 24 h. Subsequently, cells were washed with PBS, and then incubated with Hoechst 33342 at room temperature for 10 min. The cells were then observed by inverted microscope or fluorescent microscope.

Western blotting.[42] After 48 h treatment, total protein was extracted using centrifuging at 13 000g at 4 °C for 10 min, and then determined using BCA Protein Assay kit. The proteins were separated by 10% SDS-PAGE, and then transferred to a nitrocellulose membrane, which was blocked with 5% skim milk for 2 h and incubated with primary antibodies: CDK1, CDK2, CyclinA, CyclinB1, cleaved caspase 3, cleaved caspase 8, cleaved caspase 9, VEGFR-2, MMP-2, E-cadherin, TopoIIα, TopoIIβ, COX-2, iNOS, p-ERK1/2, p-AKT, p-STAT3 and β-actin overnight at 4 °C. After washing, membranes were then treated with secondary antibodies at room temperature for 2 h. The immunoreactive bands were visualized using enhanced chemiluminescence detection system and quantitated with using Gel-Pro32 software.

Wound healing assay. MUM-2B cells were seeded in a 6 well plate for 24 h, and then washed with PBS to remove floated and detached cells and photographed (0 h). MUM-2B cells were successively incubated with 0.1% DMSO and test compounds at the indicated concentration for 24 h. Wounded areas were photographed under an inverted microscope (OLYMPUS, IX51) at 100× magnification.

Conclusions

In summary, two novel conjugates of podophyllotoxin–pterostilbene were synthesized and evaluated against human uveal melanoma cell lines *in vitro*. Compound **B1** exhibited a significant IC$_{50}$ value of 0.081 ± 0.004 μM against MUM-2B cells. Treatment with **B1** induced MUM-2B cell cycle arrest at S phase and apoptosis, as well as showed antimigratory activity. Furthermore, **B1** significantly inhibited TOPOIIα and TOPOIIβ expression, simultaneously, suppressed the ERK1/2 and AKT pathways in MUM-2B cells. The antitumor mechanisms of **B1** were presented in Fig. 11. Overall, our findings indicated that conjugate **B1** might be a potent antineoplastic agent for uveal melanoma chemotherapy, however, metabolic stability evaluation and anticancer efficacy *in vivo* of conjugates still need our further studies.

Acknowledgements

Notes and references

1 A. D. Singh, M. E. Turell and A. K. Topham, *Ophthalmology*, 2011, **118**, 1881–1885.

2 S. E. Coupland, S. L. Lake, M. Zeschnigk and B. E. Damato, *Eye*, 2013, **27**, 230–242.

3 P. L. Blanco, L. A. Lim, C. Miyamoto and M. N. Burnier, *Melanoma Res.*, 2012, **22**, 334–340.

4 P. A. O'Neill, M. Butt, C. V. Eswar, P. Gillis and E. Marshall, *Melanoma Res.*, 2006, **16**, 245–248.

5 D. J. Newman and G. M. Cragg, *J. Nat. Prod.*, 2012, **75**, 311–335.

6 D. J. Newman and G. M. Cragg, *J. Nat. Prod.*, 2016, **79**, 629–661.

7 Y. Damayanthi and J. W. Lown, *Curr. Med. Chem.*, 1998, **5**, 205–252.

8 M. Gordaliza, P. A. García, J. M. Miguel del Corral, M. A. Castro and M. A. Gómez-Zurita, *Toxicon*, 2004, **44**, 441–459.

9 H. Xu, M. Lv and X. Tian, *Curr. Med. Chem.*, 2009, **16**, 327–349.

10 L. Bohlin and B. Rosen, *Drug Discovery Today*, 1996, **1**, 343–351.

11 Y. Q. Liu, J. Tian, K. Qian, X. B. Zhao, S. L. Morris-Natschke, Y. Liu, X. Nan, X. Tian and K. H. Lee, *Med. Res. Rev.*, 2015, **35**, 1–62.

12 Y. You, *Curr. Pharm. Des.*, 2005, **11**, 1695–1717.

13 A. Kamal, S. M. Ali Hussaini, A. Rahim and S. Riyaz, *Expert Opin. Ther. Pat.*, 2015, **25**, 1025–1034.

14 A. Kamal, A. Mallareddy, P. Suresh, V. L. Nayak, R. V. C. R. N. C. Shetti, N. S. Rao, J. R. Tamboli, T. B. Shaik, M. V. P. S. Vishnuvardhan and S. Ramakrishna, *Eur. J. Med. Chem.*, 2012, **47**, 530–545.

15 A. Kamal, J. R. Tamboli, M. V. P. S. Vishnuvardhan, S. F. Adil, V. L. Nayak and S. Ramakrishna, *Bioorg. Med. Chem. Lett.*, 2013, **23**, 273–280.

16 B. Meunier, *Acc. Chem. Res.*, 2008, **41**, 69–77.

17 A. M. Rimando, M. Cuendet, C. Desmarchelier, R. G. Mehta, J. M. Pezzuto and S. O. Duke, *J. Agric. Food Chem.*, 2002, **50**, 33453–33457.

18 E. S. Park, Y. Lim, J. T. Hong, H. S. Yoo, C. K. Lee, M. Y. Pyo and Y. P. Yun, *Vasc. Pharmacol.*, 2010, **53**, 61–67.

19 C. Stockley, P. L. Teissedre, M. Boban, C. Di Lorenzo and P. Restani, *Food Funct.*, 2012, **10**, 995–1007.

20 L. Pari and M. A. Satheesh, *Life Sci.*, 2006, **79**, 641–645.

21 A. M. Rimando, R. Nagmani, D. R. Feller and W. Yokoyama, *J. Agric. Food Chem.*, 2005, **53**, 3403–3407.

22 W. Nutakul, H. S. Sobers, P. Qiu, P. Dong, E. A. Decker, D. J. McClements and H. Xiao, *J. Agric. Food Chem.*, 2011, **59**, 10964–10970.

23 C. P. Ko, C. W. Lin, M. K. Chen, S. F. Yang, H. L. Chiou and M. J. Hsieh, *Oral Oncol.*, 2015, **51**, 593–601.

24 M. H. Pan, Y. S. Chiou, W. J. Chen, J. M. Wang, V. Badmaev and C. T. Ho, *Carcinogenesis*, 2009, **30**, 1234–1242.

25 M. J. Ruiz, M. Fernández, Y. Picó, J. Mañes, M. Asensi, C. Carda, G. Asensio and J. M. Estrela, *J. Agric. Food Chem.*, 2009, **57**, 3180–3186.

26 P. Ferrer, M. Asensi, R. Segarra, A. Ortega, M. Benlloch, E. Obrador, M. T. Varea, G. Asensio, L. Jordá and J. M. Estrela, *Neoplasia*, 2005, **7**, 37–47.

27 C. M. Remsberg, J. A. Yanez, Y. Ohgami, K. R. Vega-Villa, A. M. Rimando and N. M. Davies, *Phytother. Res.*, 2008, **22**, 169–179.

28 L. Zhang, F. Chen, J. Wang, Y. Chen, Z. Zhang, Y. Lin and X. Zhu, *RSC Adv.*, 2015, **5**, 97816–97823.

29 L. Zhang, Z. Zhang, J. Wang, Y. Chen, F. Chen, Y. Lin and X. Zhu, *RSC Adv.*, 2016, **6**, 2895–2903.

30 L. Zhang, F. Chen, Z. Zhang, Y. Chen and J. Wang, *Bioorg. Med. Chem. Lett.*, 2016, **26**, 38–42.

31 J. H. Cho, W. G. Hong, Y. J. Jung, J. Lee, E. Lee, S. G. Hwang, H. D. Um and J. K. Park, *Tumor Biol.*, 2015, **37**, 1–11.

32 K. K. Mak, A. T. Wu, W. H. Lee, T. C. Chang, J. F. Chiou, L. S. Wang, C. H. Wu, C. Y. F. Huang, Y. S. Shieh, T. Y. Chao, C. T. Ho, G. C. Yen and C. T. Yeh, *Mol. Nutr. Food Res.*, 2013, **57**, 1123–1134.

33 K. Li, S. J. Dias, A. M. Rimando, S. Dhar, C. S. Mizuno, A. D. Penman, J. R. Lewin and A. S. Levenson, *PLoS One*, 2013, **8**, e57542.

34 K. J. Huang and L. H. Sui, *Med. Oncol.*, 2012, **29**, 318–323.

35 S. Valastyan and R. A. Weinberg, *Cell*, 2011, **147**, 275–292.

36 N. Khan and H. Mukhtar, *Cancer Metastasis Rev.*, 2010, **29**, 435–445.

37 J. Ren, L. Wu, W. Q. Xin, X. Chen and K. Hu, *Bioorg. Med. Chem. Lett.*, 2012, **22**, 4778–4782.

38 C. S. Lai, J. H. Lee, C. T. Ho, C. B. Liu, J. M. Wang, Y. J. Wang and M. H. Pan, *J. Agric. Food Chem.*, 2009, **57**, 10990–10998.

39 Y. S. Chiou, M. L. Tsai, K. Nagabhushanam, Y. J. Wang, C. H. Wu, C. T. Ho and M. H. Pan, *J. Agric. Food Chem.*, 2011, **59**, 2725–2733.

40 S. Paul, A. J. DeCastro, H. J. Lee, A. K. Smolarek, J. Y. So, B. Simi, C. X. Wang, R. Zhou, A. M. Rimando and N. Suh, *Carcinogenesis*, 2010, **31**, 1272–1278.

41 L. Zhang, F. Chen, Z. Zhang, Y. Chen, Y. Lin and J. Wang, *Bioorg. Med. Chem. Lett.*, 2016, **26**, 4466–4471.

42 L. Zhang, Z. Zhang, F. Chen, Y. Chen, Y. Lin and J. Wang, *Eur. J. Med. Chem.*, 2016, **123**, 226–235.